THE JOURNAL OF BIOLOGICAL CHEMISTRY VOL. 284, NO. 40, pp. 27101–27113, October 2, 2009

A Lipid Profile Typifies the Beijing Strains of *Mycobacterium tuberculosis*

IDENTIFICATION OF A MUTATION RESPONSIBLE FOR A MODIFICATION OF THE STRUCTURES OF PHTHIOCEROL DIMYCOCEROSATES AND PHENOLIC GLYCOLIPIDS[*][S]

Received for publication, July 7, 2009 Published, JBC Papers in Press, August 2, 2009, DOI 10.1074/jbc.M109.041939

Gaëlle Huet[‡§1], Patricia Constant[‡§], Wladimir Malaga[‡§], Marie-Antoinette Lanéelle[‡§], Kristin Kremer[¶], Dick van Soolingen[¶], Mamadou Daffé[‡§], and Christophe Guilhot[‡§2]

From the [‡]Institut de Pharmacologie et de Biologie Structurale, CNRS, 205 Route de Narbonne, F-31077 Toulouse, France, [§]Université de Toulouse, Université Paul Sabatier, Institut de Pharmacologie et de Biologie Structurale, F-31077 Toulouse, France, and [¶]National Mycobacteria Reference Laboratory, National Institute for Public Health and the Environment, 3720 BA Bilthoven, The Netherlands

The *Mycobacterium tuberculosis* Beijing strains are a family highly prevalent in Asia and have recently spread worldwide, causing a number of epidemics, suggesting that they express virulence factors not found in other *M. tuberculosis* strains. Accordingly, we looked for putative characteristic compounds by comparing the lipid profiles of several Beijing and non-Beijing strains. All the Beijing strains analyzed were found to synthesize structural variants of two well known characteristic lipids of the tubercle bacillus, namely phthiocerol dimycocerosates (DIM) and eventually phenolglycolipids (PGL). These variants were not found in non-Beijing *M. tuberculosis* isolates. Structural elucidation of these variants showed that they consist of phthiotriol and glycosylated phenolphthiotriol dimycocerosates, eventually acylated with 1 mol of palmitic acid, in addition to the conventional acylation of the *β*-diol by mycocerosic acids. We demonstrated that this unusual lipid profile resulted from a single point mutation in the *Rv2952* gene, which encodes the *S*-adenosylmethionine-dependent methyltransferase participating to the *O*-methylation of the third hydroxyl of the phthiotriol and phenolphthiotriol in the biosynthetic pathway of DIM and PGL. Consistently, the mutated enzyme exhibited *in vitro* a much lower *O*-methyltransferase activity than did the wild-type Rv2952. We finally demonstrated that the structural variants of DIM and PGL fulfill the same function in the cell envelope and virulence than their conventional counterparts.

The factors contributing to the development of tuberculosis after infection with the etiologic agent of this disease, *Mycobacterium tuberculosis*, are not completely understood. It is currently thought that the genetic traits of both host and pathogen influence the outcome of the disease (1, 2). On the pathogen side, molecular epidemiological studies have differentiated clinical isolates of *M. tuberculosis* into defined genetically related lineages (3). One of the most important worldwide lineages, the "Beijing" lineage, was initially described by van Soolingen *et al.* (4) who showed that more than 85% of *M. tuberculosis* isolates from the Beijing region belong to this genetically conserved genotype. The Beijing strains were grouped together on the basis of their highly similar multicopy IS*6110* restriction fragment polymorphism patterns, the deletion of spacers 1–34 in the direct repeat region found in all *M. tuberculosis* strains, and the insertion of IS*6110* into the *dnaA-dnaN* locus (5). This genotype family of *M. tuberculosis* is highly prevalent in Southeast Asia, where more than 50% of the strains isolated correspond to the Beijing genotype (6). However, these strains have spread worldwide and have been responsible for major outbreaks of tuberculosis. The "W" strain responsible for a multidrug-resistant tuberculosis in the New York region, for example, belongs to this genotype (7, 8). A Beijing strain was introduced into Gran-Canaria Island in 1993 and rapidly spread; this strain accounted for 27.1% of tuberculosis cases on the island in 1996 (9). This spread of Beijing strains from the region of the world in which they are endemic to other areas in which they have become epidemic suggests that these strains may be more virulent than others. Consistent with this hypothesis, several studies have demonstrated that mice infected with Beijing strains die more rapidly than mice infected with other strains (10–13). This hypervirulence phenotype has been associated with a failure of Beijing strains to induce or to maintain an adequate Th1-type immune response (10, 12) and with more severe pneumonia resulting in the death of the infected animals. A recent study suggests that patients infected with Beijing strains are more likely to develop extrathoracic tuberculosis than people infected with strains of other lineages (14). This observation is consistent with the results obtained in a rabbit model with the Beijing strain HN878, which was found more likely to infect the brain and to disseminate (15). A recent study in Vietnam pointed out that the typical lineage of Beijing genotype strains is more frequently found in patients who received a Bacillus Calmette-Guérin vaccination. This sug-

* This work was supported in part by Agence Nationale de la Recherche Grant 06 MIME 037 01 and CNRS Grant MIE 2006.
[S] The on-line version of this article (available at http://www.jbc.org) contains supplemental Fig. SF1.
[1] Recipient of a Fondation pour la Recherche Medicale fellowship.
[2] To whom correspondence should be addressed: CNRS, IPBS (Institut de Pharmacologie et de Biologie Structurale), 205 Route de Narbonne, 31077 Toulouse Cedex 4, France. Fax: 33-5-61-17-55-80; E-mail: Christophe.Guilhot@ipbs.fr.

gests that bacteria of this lineage are more capable of circumventing Bacillus Calmette-Guérin-induced immunity (16).

In the case of the HN878 strain, the production of a phenolic glycolipid (PGL)[3] was shown to be important for the hypervirulent phenotype. The disruption of *pks15/1*, a PGL biosynthetic gene (17), in strain HN878 increased the release of pro-inflammatory cytokines by infected murine bone marrow macrophages and decreased the virulence of the bacterium in the mouse and rabbit disease models (13, 15). PGL are very unusual molecules with a lipid core and a saccharide domain. The lipid core is formed by a long chain β-diol, naturally occurring as a diester of polymethyl-branched fatty acids and common to phthiocerol dimycocerosates (DIM), another group of lipids found in the cell envelope of *M. tuberculosis* and a few other slow-growing *Mycobacterium* species (18) (Fig. 1*A*). In the major form of PGL from *M. tuberculosis* (PGL-tb), this lipid core is ω-terminated by an aromatic nucleus glycosylated with a 2,3,4-tri-*O*-methyl-L-fucopyranosyl-(α1→3)-L-rhamnopyranosyl-(α1→3)-2-*O*-methyl-L-rhamnopyranosyl-(α1→) (19) (Fig. 1*A*). This structure is specific to *M. tuberculosis* and *Mycobacterium canettii* (18, 20). Only a few *M. tuberculosis* strains synthesize PGL-tb because of a natural frameshift mutation in the *pks15/1* gene (17). Thus, based on the results of Reed *et al.* (13), it was thought that the production of this glycolipid was the principal cause of hypervirulence in Beijing strains. However, even within the Beijing lineage, only a minority of isolates produce PGL-tb (21, 22). In addition, complementation of the laboratory strain H37Rv with a functional *pks15/1* allele, allowing the production of PGL-tb, does not significantly increase the virulence of this strain in the mouse and rabbit models (22). The molecular reasons for the higher virulence of strains of the Beijing lineage therefore remain unclear.

In this study, we identified a mutation specific to the Beijing lineage that affected the activity of an enzyme involved in PGL-tb and DIM biosynthetic pathways. We analyzed the impact of this mutation on the structure of these compounds and explored the potential changes in cell envelope function and virulence induced by this mutation.

EXPERIMENTAL PROCEDURES

Bacterial Strains, Growth Media, and Culture Conditions—*M. tuberculosis* Beijing strains were obtained from the collection of the National Institute for Public Health and the Environment (Bilthoven, The Netherlands), with the exception of Beijing strains HN878 and 1237 that were kindly provided by Prof. Clifton Barry III (Tuberculosis Research Section, National Institutes of Health, Rockville, MD) and Prof. Carlos Martin (Grupo de Genetica de Micobacterias, Universidad de Zaragoza, Spain) respectively. *M. tuberculosis* strains were grown at 37 °C in Middlebrook 7H9 broth (Invitrogen) containing ADC (0.2% dextrose, 0.5% bovine serum albumin fraction V, 0.0003% beef catalase) and 0.05% Tween 80 when necessary, and on solid Middlebrook 7H11 broth containing OADC (ADC plus 0.005% oleic acid). When required, kanamycin (Km) and hygromycin (Hyg) were used at concentrations of 40 and 50 $\mu g \cdot ml^{-1}$, respectively. Plasmids were propagated at 37 °C in *Escherichia coli* DH5α in LB broth or LB agar (Invitrogen) supplemented with either Km (40 $\mu g \cdot ml^{-1}$) or Hyg (200 $\mu g \cdot ml^{-1}$).

Sequencing of the Rv2952 Gene—Genomic DNA was used as the template for PCR amplification of the *Rv2952* gene with specific primers binding 91 bp upstream and 64 bp downstream from the *Rv2952* gene as follows: 2952 forward (5′-GGATGTCATGGCATCGACCG-3′) and 2952 reverse (5′-ATATAGAACGATGTCGAACTCG-3′). The PCR was performed on a GeneAmp PCR System 2700 thermocycler (Applied Biosystems) in a final volume of 50 μl containing 2.5 units of *Taq*DNA polymerase (New England Biolabs), 10% DMSO, and 1 μM of each primer. Reactions were initiated by denaturation for 5 min at 94 °C, and primer extension was then carried out over 30 cycles of denaturation for 30 s at 94 °C, annealing for 30 s at 57 °C, and extension for 1 min at 72 °C. A final extension of 10 min at 72 °C was then applied. PCR products were analyzed by electrophoresis in a 0.8% agarose gel. The 968-bp fragment was purified with the QIAquick purification kit (Qiagen, Courtaboeuf, France) and inserted into the pGEM®-T vector (Promega). Sequencing was carried out by Millegen (Labège, France) with the SP6 and T7 primers.

Construction of the Rv2952 Complementation Vectors and the M. tuberculosis H37Rv and Beijing Complemented Strains—A region covering the *Rv2952* gene, from 500 bp upstream from the start codon to 8 bp downstream from the stop codon, was amplified by PCR from the *M. tuberculosis* H37Rv and HN878 strains with the primers Rv2952M (5′-TATATGACGTCGGATTGCGCCGACCTGCA-3′) and Rv2952N (5′-TATATACTAGTCAGTCCTTGGTGAAGCAGTA-3′). The PCR products were purified, digested with AatII and SpeI, and inserted between the AatII and SpeI sites of pMIP12d vector (20). The inserts were recovered from these plasmids as AatII-NheI fragments containing the transcription terminator ESAT 6. These fragments were inserted into AatII + NheI-digested pMV361 vector to give rise to p2952wt and p2952mu. These plasmids were transferred alone or with pPET1 into H37Rv, HN878, and 94-1707 cells by electroporation. Transformants were selected onto 7H11 plates supplemented with OADC, Km, and Hyg when required.

Production of Rv2952 in E. coli and Enzymatic Assays—The Rv2952 or Rv2952 G176R proteins were produced in *E. coli* using a T7 promoter expression system. The corresponding genes were cloned upstream in a His tag coding sequence in plasmid pET26b (Novagen). *E. coli* BL21(DE3) strains were transformed with each construct and the empty vector and grown in 10 ml of LB medium supplemented with antibiotics. At an $A_{600\ nm}$ of 0.4, expression of Rv2952 (or the mutated protein) was induced by adding 0.1 mM isopropyl 1-thio-β-D-galactopyranoside and a further incubation for 6 h at 20 °C. Cells were collected by centrifugation, and stored at −20 °C. After thawing at room temperature, cells were resuspended in 1 ml of buffer (50 mM Tris-HCl, pH 8) and sonicated using a Vibra cell apparatus (Bioblock Scientific), three times for 20 s (microtip 4, 50% duty cycle), in ice. The cleared lysates were

[3] The abbreviations used are: PGL, phenolglycolipid; DIM, phthiocerol dimycocerosates; Hyg, hygromycin; Km, kanamycin; MALDI-TOF, matrix-assisted laser desorption-ionization time-of-flight; cfu, colony-forming unit; ELISA, enzyme-linked immunosorbent assay; TNF-α, tumor necrosis factor-α; IL, interleukin; BMDM, bone marrow-derived macrophage; MIC, minimal inhibitory concentration.

obtained following centrifugation at 12,000 × *g* for 15 min. Protein concentration was assayed using the method of Bradford (Bio-Rad protein assay), and the amounts of Rv2952 and Rv2952 G176R proteins in these extracts were evaluated by Western blot using anti-His antibodies (Rockland), revelation with ECL Western blotting detection system (GE Healthcare), and quantification of the signal using GS800 calibrated densitometer and Quantity One 4.6.3 software (Bio-Rad).

Two substrates were used for *O*-methyltransferase activity as follows: the phthiotriol dimycocerosates prepared from *M. tuberculosis*, the natural substrate of the enzyme, and the 2-hexadecanol (Aldrich) chosen for its structural analogy with phthiocerol and relatives, especially phthiocerol B (18) and for the putative solubility problem with very long chain compounds as the C80–90 DIM-like compounds in *in vitro* tests. The lipids were dissolved at 60 mM for 2-hexadecanol and 1.5 mM for phthiotriol dimycocerosates in dimethyl sulfoxide, and *S*-[*methyl*-^{14}C]adenosyl-L-methionine, specific activity 50.43 mCi·mmol^{-1} (PerkinElmer Life Sciences), was used as a tracer. The assay buffer was 50 mM Tris-HCl, pH 8.

Briefly, in a final volume of 275 μl, 50–200 μl of protein crude extracts (0.5 mg·ml^{-1}) were incubated at 37 °C for 1 h under agitation (200 rpm) in the presence of lipid substrates (10 μl) and *S*-[*methyl*-^{14}C]adenosyl-L-methionine (28 μl). The reaction was stopped by adding a few drops of 20% H_2SO_4, and the reaction products were extracted three times with diethyl ether. The upper organic phases were pooled, washed with water until neutrality, and dried under air stream. The whole resulting material, dissolved in diethyl ether (30 μl), was spotted on TLC and run with petroleum ether/ether 9:1 (v/v) before exposure to Typhoon Imager (Amersham Biosciences) for the detection of labeled lipids. In initial experiments, kinetics of product formation was determined by stopping the reaction at 5, 10, 15, 20, 30, and 60 min and 6 h (data not shown). The incubation time (1 h) of subsequent experiments was chosen because the reaction was in initial velocity phase.

DIM and PGL Labeling, Extraction, and Purification—Each strain was cultured (16 ml) to exponential growth phase and labeled by incubation with 0.625 μCi·ml^{-1} [1-^{14}C]propionate (specific activity of 54 Ci·mol^{-1}) for 24 h with continuous shaking. Lipids were extracted by adding 2 volumes of CH_3OH and 1 volume of $CHCl_3$ to 0.8 volume of culture, to yield a homogeneous one-phase mixture. After incubation for 2 days, the mixture was partitioned into two phases by adding 1 volume of $H_2O/CHCl_3$ (1:1, v/v). The organic phase was recovered. The extraction was repeated once by adding 1 volume of $CHCl_3$ to the aqueous phase. The organic phases were pooled, washed at least twice with water, and dried before analysis. The dried lipid extracts from each culture were dissolved in 100 μl of $CHCl_3$, and 30 μl of this preparation were spotted onto a Silica Gel 60 TLC plate (20 × 20 cm; Merck). The TLC plate was run in $CHCl_3/CH_3OH$ (95:5, v/v) or in petroleum ether/diethyl ether (90:10, v/v) for PGL and DIM analysis, respectively. Labeled lipids were visualized with a Typhoon PhosphorImager (Amersham Biosciences). The production of various PGL and DIM forms was quantified by comparing the number of counts/min obtained for the lipid of interest with the total number of counts/min spotted. As the various PGL and DIM forms produced in the same batch of culture are expected to be labeled at the same position and with the same efficiency, comparison of this ratio provided a good evaluation of the relative amount of each DIM and PGL variant. For nonradioactive analysis, bacterial cells were harvested from 125-ml cultures in Sauton's medium, and lipids were extracted by a first incubation in $CHCl_3/CH_3OH$ (1:2, v/v) for 2 days at room temperature and then in $CHCl_3/CH_3OH$ (2:1, v/v). The two organic phases were pooled, washed twice with water, and dried before analysis. Extracted mycobacterial lipids were analyzed by TLC after resuspension in $CHCl_3$ at a final concentration of 20 mg·ml^{-1}. Equivalent amounts of each extract were spotted on TLC plates. DIM and PGL were visualized by spraying the plates with 10% phosphomolybdic acid in ethanol or with a 0.2% anthrone solution in concentrated H_2SO_4, respectively, followed by heating. For structural analysis, lipids were fractionated by chromatography on a Florisil column. Increasing concentrations of diethyl ether in petroleum ether or CH_3OH in $CHCl_3$ were used as eluents to obtain various members of the DIM and PGL family, respectively. The fractions containing the product of interest were then pooled and separated on preparative TLC. An enriched fraction was then finally recovered by scraping the silica gel from the plates.

Structural Analysis—Purified molecules were analyzed by matrix-assisted laser desorption-ionization time-of-flight (MALDI-TOF) mass spectrometry, as described previously (23). Spectra were acquired in reflectron mode, with an Applied Biosystems 4700 analyzer mass spectrometer (Applied Biosystems, Framingham) equipped with an Nd:YAG laser (wavelength 355 nm; pulse <500 ps; repetition rate 200 Hz). A total of 2500 shots were accumulated in positive ion mode, and mass spectrometry data were acquired with the default calibration for the instrument. NMR spectroscopy experiments were carried out at 295 K on a Bruker AVANCE spectrometer operating at 600,13 MHz with a 5-mm triple resonance TCI ^{1}H ^{13}C ^{15}N pulsed field z-gradient cryoprobe. Samples were dissolved in 99.9% $CDCl_3$. Chemical shifts are expressed in parts/million using the chloroform signal as an internal reference (7.23 ppm).

SDS Resistance Assays—Cultures of strains used for SDS resistance assays were grown to mid-exponential growth phase in 7H9 supplemented with ADC, 0.05% Tween 80, and Km when necessary. Cultures were centrifuged at 10,000 × *g* for 10 min at room temperature in a Jouan CR412 centrifuge with a T4 swing out rotor. The cells were then resuspended in 7H9-ADC without Tween 80 and incubated at 37 °C for 48 h. Bacterial concentration was evaluated by measuring the absorbance at 600 nm, and 10-ml cultures were inoculated to a final A_{600} of 0.02. SDS was added to each culture at a final concentration of 0.1%. Aliquots were collected after 0, 1, 4, and 8 days of growth, and the number of viable bacteria remaining was evaluated by plating serial dilutions on solid medium.

Drug Sensitivity—Bacteria were prepared 48 h before plating from frozen stocks of known concentrations. Stocks were centrifuged and bacteria were resuspended in 7H9 and incubated at 37 °C for 2 days. Serial dilutions were then plated on 7H11 containing various concentration of rifampicin, isoniazid, or ethambutol and incubated for 3–4 weeks at 37 °C. For all the drugs tested, the minimal inhibitory concentration (MIC) cor-

responded to the minimal drug concentrations resulting in decreases of more than 90% in cfu counts.

Competition Assays in Mice—For the mixed infection experiments in mice, the *M. tuberculosis* HN878 and 94-1707 wild-type strains were transformed with the modified mycobacterial plasmid pMV361Hy derived from the pMV361 plasmid in which the Km resistance cassette was replaced by a Hyg resistance marker. The inoculum was prepared by mixing HN878:pMV361Hy cells with HN878:p2952wt cells, or 94-1707: pMV361Hy/94-1707:p2952wt, at a final concentration of 2.5×10^6 cfu·ml^{-1} for each strain. The concentration of the inoculum was determined by plating serial dilutions on 7H11 plates containing either Km or Hyg. Fifteen BALB/c mice were infected intranasally with 20 μl (1×10^5 cfu) of the inoculum, and for each infection group, five mice from each group were killed 1, 21, and 42 days after infection, and the numbers of colony-forming units present in lungs and spleen (except for day 1 after infection) were determined by plating serial dilutions on 7H11 plates containing either Km or Hyg serial dilutions of homogenates obtained from the organs by homogenizing tissues in 5 ml of NaCl/P_i supplemented with 0.05% Tween 80. All investigations in mice were carried out in accordance with CNRS guidelines for animal experimentation and were approved by the "Comité Regional d'Ethique pour l'Expérimentation Animale."

Cytokine Experiments—We generated bone marrow-derived macrophages (BMDM) by flushing bone marrow cells from the femurs of ~8-week-old B6D2 F_1 mice into high glucose Dulbecco's modified Eagle's medium (Invitrogen) supplemented with 20% heat-inactivated fetal calf serum (Dutscher), 10% L929 conditioned medium, and 2 mM glutamine. For the infection assays, mouse bone marrow cells were seeded at a density of 2×10^5 cells per well in 24-well plates and allowed to differentiate for 7 days. Bacteria used for the infection were

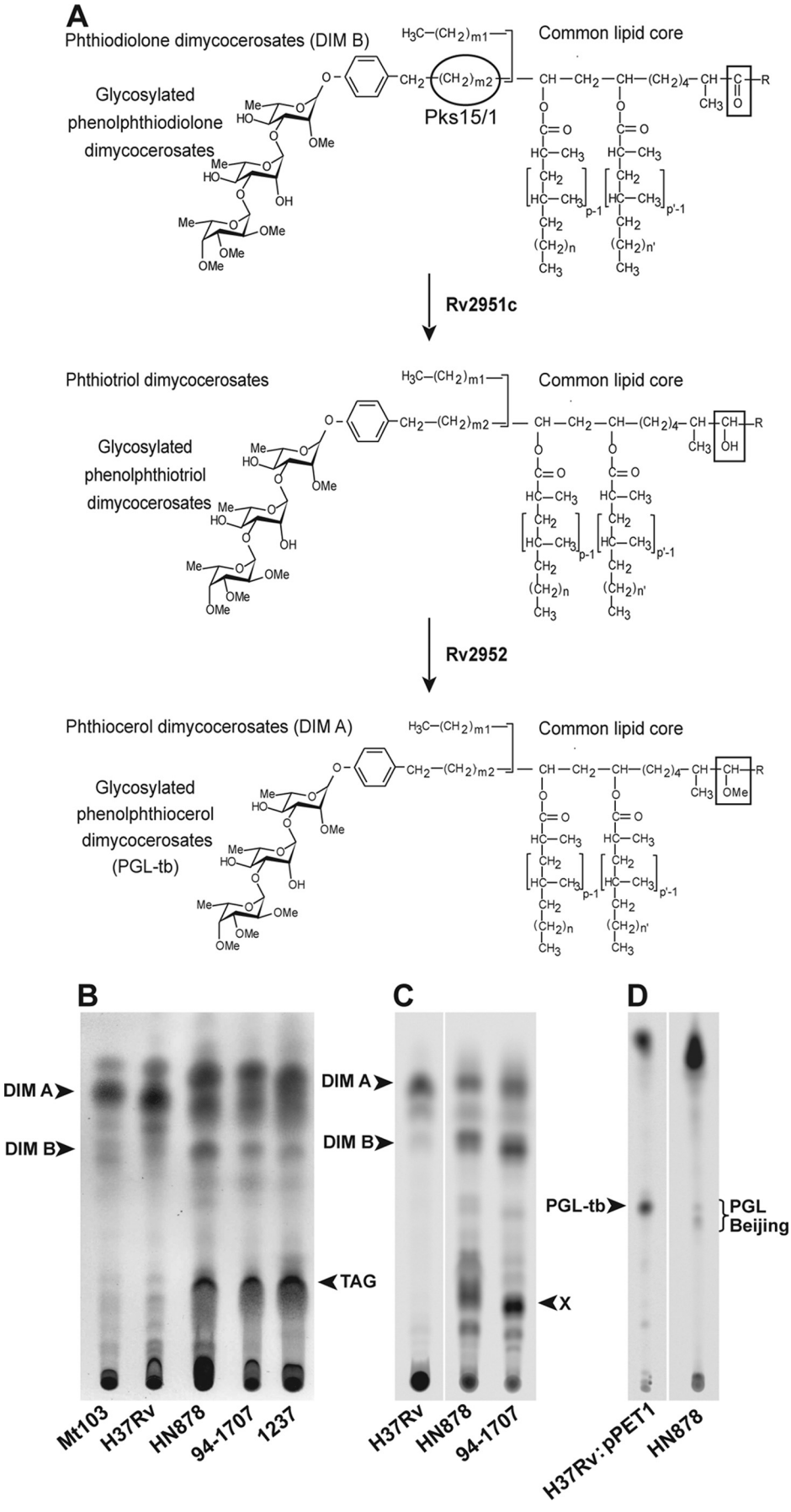

freshly prepared in Dulbecco's modified Eagle's medium supplemented with 20% fetal calf serum and 2 mM glutamine. Bacterial concentration was adjusted to a final concentration of 3.3×10^6 bacteria per ml on the basis of absorbance 600 nm. An aliquot of the *M. tuberculosis* suspensions used to infect macrophages was spread on 7H11 plates to determine the number of bacteria in the inoculum more precisely. Infection assays were carried out as follows. The culture medium of each well was removed, and the cells were washed once with 500 μl of phosphate-buffered saline. We then added 300 μl of the mycobacterial suspension to obtain a multiplicity of infection of 5:1 (bacilli/BMDM). Control wells containing uninfected macrophages were filled with 300 μl of fresh medium. Infected and uninfected cultures were incubated for 4 h at 37 °C in an atmosphere containing 5% CO_2. Infection was terminated by removing the overlaying medium and washing each well three times with 500 μl of Dulbecco's modified Eagle's medium before adding 400 μl of fresh culture medium per well. At 5 and 24 h the supernatants were recovered and analyzed for the presence of TNF-α, IL-10, IL-12p70, and MCP-1 by enzyme-linked immunosorbent assay (ELISA) (R & D Systems).

Statistical Analysis—Statistical analysis of the data were carried out with a one-way analysis of variance test to determine the significance of differences between the cytokine levels.

RESULTS

Structural and Quantitative Analyses of DIM and PGL Produced by Beijing Strains—M. tuberculosis strains are known to produce species-specific lipids that are critical for their virulence (24, 25); among these are the phthiocerol dimycocerosates (DIM A) and relatives (DIM B) (Fig. 1*A*). Some strains also elaborate the structurally related glycosylated phenolphthiocerol dimycocerosates (PGL-tb; Fig. 1*A*). These variants have different mobilities on TLC, and thus their production can be analyzed by this method. TLC analysis of the lipids of various clinical isolates of *M. tuberculosis* showed a special lipid profile for the Beijing isolates, particularly in the migration area of DIM (Fig. 1*B*) and PGL (data not shown). Phthiocerol dimycocerosate (DIM A) was the major constituent in H37Rv and other non-Beijing isolates but appeared to be less abundant in Beijing strains (Fig. 1*B*). In contrast, other compounds migrating at the R_f of phthiodiolone dimycocerosates (DIM B) or triglycerides were more abundant in Beijing isolates than in non-Beijing *M. tuberculosis* strains. Similarly, PGL extracted from HN878 gave two closely migrating spots, whereas only one spot was observed for PGL-tb extracted from H37Rv::pPET1, an H37Rv derivative rendered competent for PGL-tb production by the transfer of a functional copy of the *pk15/1* gene (data not shown). Although the accumulation of triglycerides in Beijing strains has been described previously (21), the modification we observed in the pattern of DIM and PGL produced by Beijing strains was not previously reported. Our observations suggested possible structural differences between the profile of DIM and PGL produced by Beijing strains and those produced by the reference strain H37Rv.

TABLE 1

Quantification of DIM labeled with [1-^{14}C]propionate in various *M. tuberculosis* strains wild-type or recombinant for the *Rv2952* gene

	% of labeled lipids[a]		
	DIM A	DIM B	X (phthiotriol dimycocerosates)
	%	%	%
A. *M. tuberculosis* strain			
H37Rv	37.6 ± 8.4	3.1 ± 1.5	
94-1707	13.0 ± 5.2	20.3 ± 3.3	30.8 ± 0.4
94-1707:p2952wt	45.7 ± 3.5	11.0 ± 2.3	
94-1707:p2952mu	14.8 ± 1.3	16.8 ± 0.6	25.1 ± 0.6
94-1707:pMV361	9.0 ± 0.3	15.0 ± 1.5	27.1 ± 1.7
HN878	11.1 ± 0.9	13.0 ± 0.5	27.9 ± 1.3
HN878:p2952wt	41.5 ± 3.3	8.0 ± 0.1	
HN878:p2952mu	16.8 ± 2.7	17.3 ± 4.9	12.3 ± 4.4
HN878:pMV361	14.6 ± 1.6	15.2 ± 6.5	14.3 ± 0.8
B. *M. tuberculosis* strain			
PMM62:p2952wt	38.6 ± 8.6	28.7 ± 18.4	
PMM62:p2952mu	20.8 ± 7.0	36.2 ± 22.1	12.1 ± 8.6
PMM62:pMV361		38.5 ± 18.5	24.1 ± 5.7
PMM62:pPET1:p2952wt	23.5 ± 3.3	10.2 ± 7.1	
PMM62:pPET1:p2952mu	7.0 ± 2.6	11.9 ± 8.7	7.3 ± 4.0
PMM62:pPET1:pMV361		14.2 ± 8.7	11.7 ± 3.7

[a] The values shown are the means ± S.D. of two independent experiments.

The following two Beijing strains were selected for further analysis: HN878, which produces both DIM and PGL, and 94-1707, which produces only DIM. The lipids produced by both strains were quantified by labeling cells with [1-^{14}C] propionate, a precursor known to be incorporated into methyl-branched fatty acid-containing lipids, such as DIM and PGL. TLC analysis of the resulting labeled lipids confirmed that the profiles of DIM produced by both Beijing strains differed from that of H37Rv (Fig. 1*C*). Indeed, although DIM A was the major compound in H37Rv (DIM A 37.6 ± 8.4% and DIM B 3.1 ± 1.5% of the labeled lipids), the amounts of compounds migrating like DIM A were similar to that of DIM B in HN878 (DIM A region 11.1 ± 0.9% and DIM B region 13.0 ± 0.5%) and 94-1707 (DIM A region 13.0 ± 5.2% and DIM B region 20.3 ± 3.3%) (Fig. 1*C* and Table 1). In addition, a major unknown compound absent from H37Rv was detected (Fig. 1*C, spot X*). This probably differs from triglycerides because the labeling was performed with [1-^{14}C]propionate. Labeling also confirmed a difference in the profiles of PGL produced by the different strains. Indeed, H37Rv::pPET1 synthesized a single form of PGL-tb, whereas HN878 produced small amounts of two PGL-like variants (Fig. 1*D*).

We further characterized the DIM-like substances produced by the two Beijing strains. Lipids exhibiting R_f values similar to

FIGURE 1. **DIM and PGL profile in *M. tuberculosis* Beijing strains.** *A,* structure of phthiocerol dimycocerosates and related compounds in *M. tuberculosis* and role of Rv2951c and Rv2952 enzymes in the last steps of DIM and PGL formation. In *M. tuberculosis, p*, *p′* = 3–5; *n*, *n′* = 16–18; *m1* = 20–22; *m2* = 15–17; *R* = -CH_2-CH_3 or -CH_3. *B,* TLC analysis of lipid extracts from bacterial cells of H37Rv, Mt103, HN878, 94-1707, and 1237 strains. Lipid extracts were dissolved in $CHCl_3$ and run in petroleum ether/diethyl ether (90:10) for DIM analysis. Lipids were visualized by spraying the TLC plate with 10% phosphomolybdic acid in ethanol, followed by heating. The positions of DIM A, DIM B, triglycerides (*TAG*) are indicated. *C* and *D,* TLC analysis of lipid extracts from [^{14}C]propionate-labeled bacterial cell of H37Rv, H37Rv:pPET1, HN878, and 94-1707. Lipid extracts were dissolved in $CHCl_3$ and run in petroleum ether/diethyl ether (90:10) for DIM analysis (*C*) and in $CHCl_3$/CH_3OH (95:5) for PGL analysis (*D*). Lipids were visualized with a Typhoon PhosphorImager. Positions of DIM A, DIM B, compounds X, and PGL are indicated.

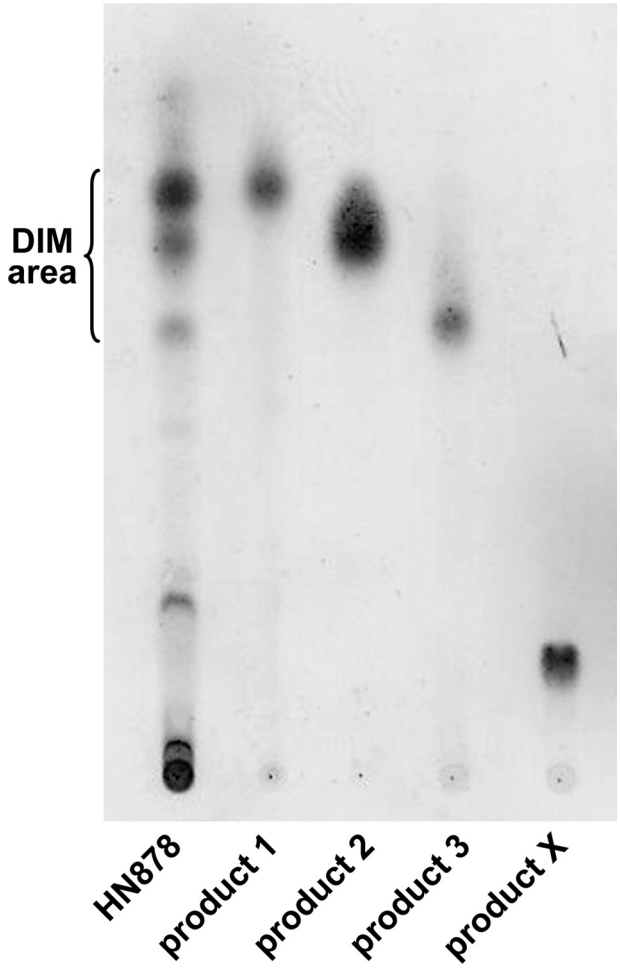

FIGURE 2. **TLC analysis of the compounds purified from Beijing strain HN878.** The enriched fractions were dissolved in $CHCl_3$ and run in petroleum ether/diethyl ether (90:10) for DIM analysis.

those of DIM A, DIM B, and compound X were first separated on a Florisil column and then further enriched by preparative TLC of the column fractions (Fig. 2). The enriched fractions were analyzed by MALDI-TOF mass spectrometry and ^{1}H NMR. The fractionation of lipids from both HN878 and 94-1707 led to two compounds (products 1 and 2) with mobilities on TLC similar to that of DIM A (Fig. 2). The mass spectrum of product 1 showed a series of pseudomolecular ion ($M + Na^+$) peaks at *m*/*z* 1642, 1656, 1670, 1684, 1698, 1712, 1726, and 1740 (Fig. 3*A*) (the major homologs are underlined). The spectrum of product 2 corresponded to that of DIM A, with a series of pseudomolecular ion ($M + Na^+$) peaks at *m*/*z* 1390, 1404, 1418, 1432, 1446, 1460, 1474, 1488, and 1502 (Fig. 3*B*). These mass values are 224 mass units lower than those observed in the mass spectrum of product 1. The mass spectrum of the product 3, exhibiting an R_f value in the region of DIM B, showed two series of pseudomolecular ion ($M + Na^+$) peaks. One corresponded to compounds of the DIM A family, whereas the other series of peaks were seen at *m*/*z* 1402, 1416, 1430, 1444, 1458, 1472, and 1486 (Fig. 3*C*), as expected for DIM B (26). Finally, product X gave a series of pseudomolecular ion ($M + Na^+$) peaks at *m*/*z* 1376, 1390, 1404, 1418, 1432, 1446, 1460, 1474, and 1488 (Fig. 3*D*). These mass values belong to the same family as the one observed for DIM A. However, the lower mobility of product X (Fig. 1*C*) suggested that it might be phthiotriol dimycocerosates, a compound previously observed in an H37Rv mutant deficient for the methylation of the hydroxyl group during the formation of DIM A (27). For phthiotriol dimycocerosates, the expected mass values are 14 mass units lower than those of DIM A and are therefore difficult to differentiate from that of DIM A because of the occurrence of homologs in the aliphatic chain length, which gave peaks differing one another by 14 mass units. We also speculated that the free hydroxyl group of the putative phthiotriol dimycocerosates would be esterified by a fatty acid, with an acyl moiety corresponding to a palmitoyl residue, to form product 1. We tested these hypotheses by carrying out ^{1}H NMR analyses on the purified products (Fig. 4). For products 2 and 3, all the proton signal resonances expected for DIM A and DIM B, respectively, were detected (Fig. 4). The spectrum obtained for product 1 (Fig. 4) included most of the proton signal resonances obtained with DIM A. However, the 3.31 and 2.82 ppm signals were absent from this spectrum. These signals correspond to the proton resonances of the methoxyl group and the methine proton of the carbon bearing this group, respectively. Instead, an additional signal was observed at 4.68 ppm (Fig. 4, *signal c2*). This signal, absent from the spectra of both DIM A and DIM B, corresponds to the methine proton resonance of a carbon bearing an esterified hydroxyl group. Overall, the mass spectrometry and NMR analyses indicated that product 1 was assignable to acylated phthiotriol dimycocerosates. The ^{1}H NMR spectrum for product X was also similar to that of DIM A except that it lacked two signals at 3.31 and 2.82 ppm and had an additional broad signal at 3.30 ppm (Fig. 4*A*, *signal c3*). The c3 signal corresponds to the proton resonance of methine bearing a hydroxyl group. Thus, the ^{1}H NMR spectrum of compound X clearly indicated that this lipid corresponded to phthiotriol dimycocerosates. These results indicated that HN878 and 94-1707 produce at least four DIM-like compounds as follows: DIM A, DIM B, and two new apolar lipids corresponding to phthiotriol dimycocerosates and acylated phthiotriol dimycocerosates.

We carried out similar analysis on the PGL produced by HN878. The various forms were purified and then analyzed by MALDI-TOF mass spectrometry and ^{1}H NMR spectroscopy. The mass spectra of the purified compounds (data not shown) led to the identification of PGL-tb and three other glycolipids. The spectrum of one of the new glycolipids showed pseudomolecular peaks 14 mass units lower than those of PGL-tb. The spectrum of the second product exhibited pseudomolecular peaks 16 mass units lower than those of PGL-tb, and the spectrum of the last compound contained peaks 224 mass units higher. Therefore, as for DIM, we presumed that the first glycolipid corresponds to glycosylated phenolphthiotriol dimycocerosates with a free hydroxyl group, and the second compound was considered to be glycosylated phenolphthiodiolone dimycoserosates (Fig. 1*A*), and the third product to be glycosylated was phenophthiotriol dimycocerosates esterified with a palmitoyl residue. Again ^{1}H NMR spectroscopy was used for the structural characterization of the PGL from HN878. The ^{1}H NMR spectra obtained with the various PGL confirmed that the

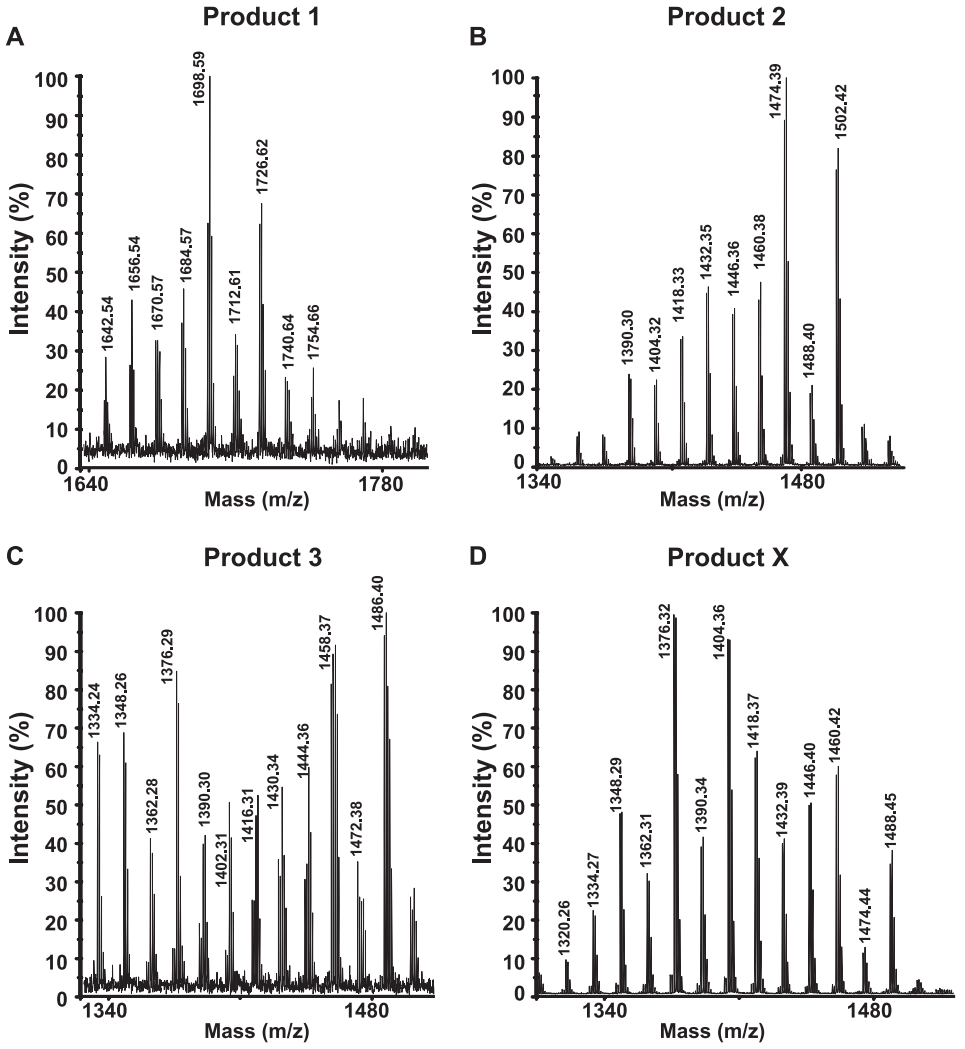

FIGURE 3. **MALDI-TOF mass spectra of product 1 (*A*), product 2 (*B*), product 3 (*C*), and product X (*D*) from *M. tuberculosis* HN878.**

HN878 strain synthesized variants of PGL structurally to those reported above for DIM (Fig. 4).

Identification of a Point Mutation Specific to the Beijing Genotype in a Gene Involved in DIM and PGL Biosynthesis—The pattern of PGL and DIM produced by the two Beijing isolates analyzed was very similar to that previously obtained for an H37Rv strain (and H37Rv expressing a functional *pks15/1* gene) with a mutation in the *Rv2952* gene, which encodes the methyltransferase catalyzing the transfer of a methyl group to the lipid moiety of DIM and PGL (27). This observation led us to examine in greater detail the sequence of the *Rv2952* ortholog from Beijing strains. This gene was amplified from the various strains by PCR and sequenced. The nucleotide sequences obtained were compared with that of the H37Rv *Rv2952* gene, and a point mutation at position 526, in which a guanine was replaced by an adenine residue, was identified. This nucleotide mutation leads to an amino acid change at codon 176, with the replacement of a glycine by an arginine residue in both the HN878 and 94-1707 strains.

We then investigated whether the $Rv2952^{G526A}$ point mutation was specific to the Beijing lineage. We amplified 28 *Rv2952* orthologs from Beijing strains selected to represent the diversity of the *M. tuberculosis* Beijing family (Table 2) and sequenced them. The nucleotide sequences of these orthologs were compared with those from seven non-Beijing *M. tuberculosis* (Table 2). The $Rv2952^{G526A}$ point mutation was found in all the Beijing strains tested, which includes ancestral ones (Table 2). By contrast, this nucleotide position was unchanged in the *Rv2952* orthologs from all the non-Beijing *M. tuberculosis* strains tested. We extended our analysis to *Rv2952* orthologs from more distant *Mycobacterium* strains, from species such as *Mycobacterium leprae* and *Mycobacterium ulcerans* in which the $Rv2952^{G526A}$ point mutation was not found.

Role of the $Rv2952^{G526A}$ Mutation in the Unusual Profiles of DIM and PGL Produced by Beijing Strains—We investigated the possible role of the $Rv2952^{G526A}$ mutation in the accumulation of structural variants of DIM and PGL in the Beijing strains by complementing the mutation. A wild-type and a mutated copy of the *Rv2952* gene, amplified by PCR from the H37Rv and HN878 genomes, respectively, were inserted separately into the integrative mycobacterial plasmid pMV361 (28). The resulting constructs, and the control plasmid carrying no gene, were used to transform HN878 and 94-1707. Two series of recombinant strains were then generated, each consisting of one recombinant strain carrying two copies of the Beijing allele of *Rv2952*, one recombinant strain carrying one Beijing allele and one non-Beijing allele, and one strain carrying the control vector, pMV361, which therefore had only the endogenous copy of *Rv2952*. The DIM contents of all the recombinant strains were then analyzed by TLC after labeling with [1-^{14}C]propionate (Fig. 5*A* and Table 3A). For the two Beijing strains carrying the control vector, HN878:pMV361 and 94-1707:pMV361, the patterns of DIM production were, as expected, similar to that of the wild-type strains (Fig. 5*A* and Table 1, part A). Similar findings were obtained for the two recombinant strains carrying the plasmid encoding the mutated *Rv2952* gene, HN878:p2952mu and 94-1707:p2952mu, which displayed profiles of DIM production similar to that of the wild-type strains. In contrast, the transfer into HN878 and 94-1707 of p2952wt, resulting in the expression of the H37Rv allele of the *Rv2952* gene, completely abolished the phthiotriol dimycocerosates accumulation and restored the production of DIM A as the major compound (45.7 ± 3.5% and 41.5 ± 3.3% of the total labeled lipids in 94-1707:p2952wt and

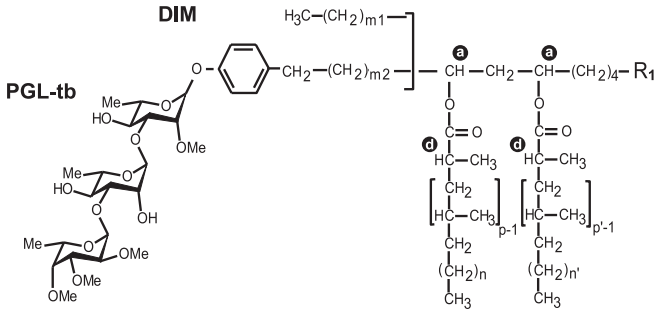

Lipids analyzed in ^{1}H-NMR

protons resonances in ppm corresponding to the main signals

	Product 1	Product 2	Product 3	Product X
a	4.81	4.81	4.81	4.81
b		3.31		
c1		2.82		
c2	4.68			
c3				3.30
d	2.49	2.49	2.49	2.49
g			1.02	
R_1 =	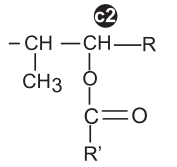	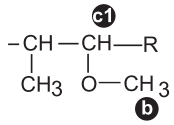	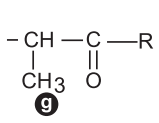	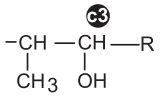
	acylated phthiotriol dimycoserosates	DIM A	DIM B	phthiotriol dimycocerosates
	glycosylated acylated phenolphthiotriol dimycocerosates	PGL-tb	glycosylated phenolphthiodiolone dimycocerosates	glycosylated phenolphthiotriol dimycocerosates

FIGURE 4. **^{1}H NMR analysis of DIM and PGL purified from *M. tuberculosis* HN878.** The *letters* on the formula indicate the proton whose resonances are given in the *table*. Structures of the analyzed compounds deduced from the ^{1}H NMR signals are represented at the *bottom* of the table. In *M. tuberculosis*, $p, p' = 3–5$; $n, n' = 16–18$; $m1 = 20–22$; $m2 = 15–17$; $R = -CH_2-CH_3$ or $-CH_3$.

HN878:p2952wt respectively), as in the reference wild-type H37Rv strain (37.6% ± 8.4) (Table 1, part A).

Labeled PGL from the HN878 series of recombinant strains were also analyzed by TLC. For HN878:pMV361 and HN878:p2952mu recombinants, the same PGL profile was obtained as for the wild-type strain HN878 (Fig. 5*B*). As expected, transformation of the HN878 strain with a wild-type copy of the *Rv2952* gene led to the reversion of the PGL profile to the non-Beijing type, in which PGL-tb is the major form (Fig. 5*B*).

These results strongly support our hypothesis that the *Rv2952*^{G526A} mutation affects the methyltransferase activity and is responsible for the unusual patterns of DIM and PGL production by Beijing strains. To confirm this finding, we replaced the wild-type *Rv2952* gene by the *Rv2952*^{G526A} allele in the laboratory strain H37Rv. For this purpose, we used the previously described H37Rv Δ*Rv2952*::*res*-Ωkm-res strain (27). The *res*-Ω*km-res* cassette was first recovered after the transient expression of the transposon γδ resolvase from plasmid pWM19 to generate strain H37Rv Δ*Rv2952*::*res* (also named PMM62). This strain was then transformed with plasmid pMV361, p2952mu, or p2952wt to generate a first series of recombinant strains. In parallel, double transformations with pPET1 in addition to pMV361, p2952mu, or p2952wt were performed to generate a second series of recombinant strains expressing a functional *pks15/1* gene and therefore competent for PGL production. The lipids produced by these six recombinant strains were labeled with [1-^{14}C] propionate (Fig. 5, *C* and *D*). As described previously for the H37Rv Δ*Rv2952*::*res*-Ωkm-res strain (27), the corresponding unmarked mutant carrying the control vector, H37Rv Δ*Rv2952*::*res*:pMV361, produced only DIM B and phthiotriol dimycocerosates (Fig. 5*C* and Table 1, part B). Complementation with the *Rv2952* allele from H37Rv led to full restoration of DIM A production (Fig. 5*C* and Table 1, part B). In contrast, H37Rv Δ*Rv2952*::*res*:p2952mu, expressing the *Rv2952*^{G526A} allele, had a DIM profile similar to that of Beijing isolates. Similar findings were obtained with the second series of strains (Table 1, part B). In addition, the PGL production profile was dependent on the *Rv2952* allele expressed by the recombinant strain; the strain expressing *Rv2952* from H37Rv produced mostly PGL-tb, whereas the strain expressing *Rv2952*^{G526A} produced the various structural variants of PGL identified in the Beijing isolate HN878 (Fig. 5*D*). Clearly, the occurrence of the *Rv2952*^{G526A} allele led to a lipid profile different from that of H37Rv or H37Rv carrying a *null* mutation in *Rv2952*. These results were entirely consistent with those obtained with the recombinant Beijing strains and demonstrated that the mutation in *Rv2952* led to a profile of DIM and PGL production different from that in non-Beijing strains.

Impact of the G176R Mutation on the Activity of Rv2952—To evaluate the expected impact of the G176R mutation on the enzymatic activity of Rv2952 suggested by the modification of the lipid profile, the wild-type and the mutated enzymes were produced in *E. coli*. Cleared lysates containing the soluble proteins were used to evaluate the *S*-adenosylmethionine-dependent methyltransferase activity on two substrates as follows: the putative substrate of this enzyme in the DIM biosynthetic pathway, *i.e.* the phthiotriol dimycocerosates, and a putatively more water-soluble and tractable compound, 2-hexa-

TABLE 2
***Rv2952*^{526} point mutation in various species of mycobacteria**

Strain	Source[a]	Species	Genotype	Country of isolation	*Rv2952*^{526}
HN878	a	*M. tuberculosis*	Beijing	United States	**A**GG Arg
210	b	*M. tuberculosis*	Beijing	United States	**A**GG Arg
1237	c	*M. tuberculosis*	Beijing	Spain	**A**GG Arg
22	d	*M. tuberculosis*	Beijing	Mongolia	**A**GG Arg
17919	d	*M. tuberculosis*	Beijing	Mongolia	**A**GG Arg
30	d	*M. tuberculosis*	Beijing	South Africa	**A**GG Arg
94-1707	d	*M. tuberculosis*	Beijing	South Africa	**A**GG Arg
44	d	*M. tuberculosis*	Beijing	Thailand	**A**GG Arg
54	d	*M. tuberculosis*	Beijing	Thailand	**A**GG Arg
90	d	*M. tuberculosis*	Beijing	South Korea	**A**GG Arg
111	d	*M. tuberculosis*	Beijing	South Korea	**A**GG Arg
113	d	*M. tuberculosis*	Beijing	Malaysia	**A**GG Arg
9401536	d	*M. tuberculosis*	Beijing		**A**GG Arg
9501317	d	*M. tuberculosis*	Beijing		**A**GG Arg
9600299	d	*M. tuberculosis*	Beijing		**A**GG Arg
9800636	d	*M. tuberculosis*	Beijing		**A**GG Arg
17383	d	*M. tuberculosis*	Beijing		**A**GG Arg
9500592	d	*M. tuberculosis*	Beijing		**A**GG Arg
17914	d	*M. tuberculosis*	Beijing		**A**GG Arg
9701445	d	*M. tuberculosis*	Beijing		**A**GG Arg
9701940	d	*M. tuberculosis*	Beijing		**A**GG Arg
9801463	d	*M. tuberculosis*	Beijing		**A**GG Arg
17002	d	*M. tuberculosis*	Beijing		**A**GG Arg
9801250	d	*M. tuberculosis*	Beijing		**A**GG Arg
9702350	d	*M. tuberculosis*	Beijing		**A**GG Arg
16362	d	*M. tuberculosis*	Beijing		**A**GG Arg
17583	d	*M. tuberculosis*	Beijing		**A**GG Arg
9801500	d	*M. tuberculosis*	Beijing		**A**GG Arg
99-0172	d	*M. tuberculosis*	Ancestral Beijing		**A**GG Arg
2003-0957	d	*M. tuberculosis*	Ancestral Beijing		**A**GG Arg
H37Rv		*M. tuberculosis*			**G**GG Gly
CDC1551	b	*M. tuberculosis*			**G**GG Gly
C	b	*M. tuberculosis*			**G**GG Gly
F11	b	*M. tuberculosis*			**G**GG Gly
2002-1611	d	*M. tuberculosis*	Hanoi		**G**GG Gly
2000-0367	d	*M. tuberculosis*	Somali		**G**GG Gly
Haarlem	b	*M. tuberculosis*	Haarlem		**G**GG Gly
AF2122/97	b	*M. bovis*			**G**GG Gly
BCG 1173P2	b	*M. bovis*			**G**GG Gly
TN	b	*M. leprae*			**G**GG Gly
Agy 99	b	*M. ulcerans*			**G**GG Gly
	e	*M. canetti*			**G**GG Gly

[a] The following sources were used: a, Prof. Clifton Barry III (Tuberculosis Research Section, National Institutes of Health, Rockville, MD); b, published genomes; c, Prof. Carlos Martin (Grupo de Genetica de Micobacterias, Universidad de Zaragoza, Spain); d, Dr. K. Kremer and D. Van Soolingen (National Institute for Public Health and the Environment, Bilthoven, The Netherlands); e, Collection of the Institut Pasteur (Paris, France).

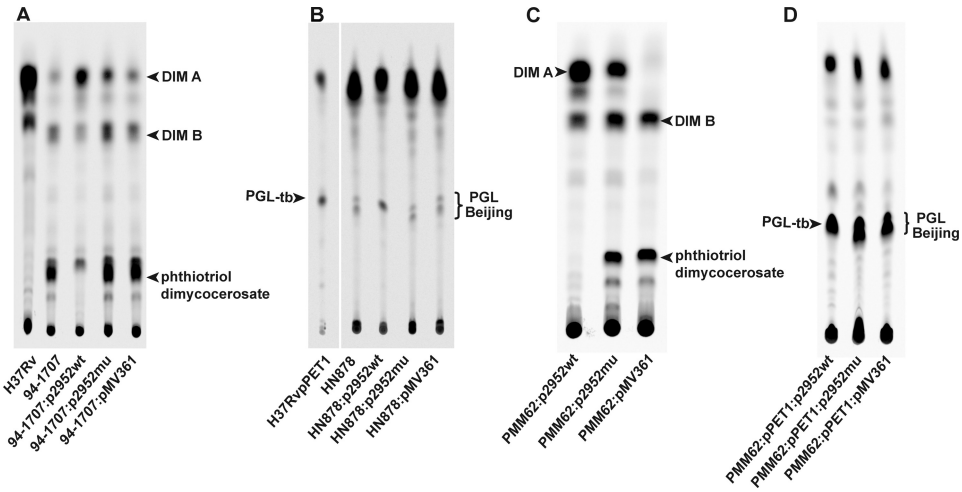

FIGURE 5. **TLC analysis of [^{14}C]propionate-labeled lipids extracted from H37Rv, HN878 wild-type and derived strains, 94-1707 wild-type and derived strains, and the PMM62-derived strains.** *A* and *C,* TLC analysis of labeled lipid extracts from bacterial cell of the H37Rv-, HN878-, and 94-1707-derived strains. Lipid extracts were dissolved in $CHCl_3$ and run in petroleum ether/diethyl ether (90:10, v/v) for DIM analysis. Lipids were visualized with a Typhoon PhosphorImager. Positions of DIM A, DIM B, and phthiotriol dimycocerosates are indicated. *B* and *D,* TLC analysis of labeled lipid extracts from bacterial cells of the H37Rv:pPET1 and HN878-derived strains. Lipid extracts were dissolved in $CHCl_3$ and run in $CHCl_3/CH_3OH$ (95:5, v/v) for PGL analysis. Lipids were visualized with a Typhoon PhosphorImager. The positions of PGL-tb and PGL Beijing are indicated.

decanol (Fig. 6*A*). For each experiment, the amount of Rv2952 or Rv2952 G176R proteins was evaluated by Western blot using anti-His antibodies (Fig. 6*B*) and signal quantification.

Cell extracts containing Rv2952 protein exhibited a very high methyltransferase activity on both 2-hexadecanol and phthiotriol dimycocerosates yielding, respectively, *O*-methyl-hexadecanol and DIM A (Fig. 6*A*). The nature of the reaction products was confirmed by co-migration with authentic standards (data not shown). When cell extracts containing similar amounts of Rv2952 G176R were used, only trace amounts of products were detected with both substrates at the highest concentration of cell extracts (Fig. 6*A*). These results demonstrated that the G176R mutation strongly affects the Rv2952

O-methyltransferase activity therefore explaining the poor production of DIM A and PGL-tb in Beijing strains.

Impact of the Rv2952^{G526A} Mutation on Cell Envelope Functions and Virulence—We previously showed that DIM are involved in the cell envelope permeability barrier and have been implicated in the resistance of the tubercle bacillus to detergent (29). Changes in resistance to detergent also provide an indication of putative perturbation of the cell envelope organization. Accordingly, we assessed the impact of the *Rv2952*^{G526A} mutation on cell envelope function by comparing the resistance to SDS of our Beijing series of mutants, which differed in their DIM and PGL profiles. All three recombinant strains derived from HN878 and the series derived from 94-1707 were cultured in the presence of 0.1% SDS. Bacterial survival was evaluated, after incubation for various periods of time with SDS, by plating serial dilutions of the culture on solid media. The three survival curves within each series were superimposable, showing that the changes in DIM and PGL profiles due to the mutation in the *Rv2952* gene had no significant effect on the resistance of *M. tuberculosis* to SDS (supplemental material).

Changes in cell envelope permeability may also affect drug diffusion, which in turn may modify the drug susceptibility of the bacterial strains. We addressed this issue by testing the two series of recombinant strains derived from HN878 and 94-1707 for their susceptibility to three major anti-tuberculous drugs. Cultures of the various strains, adjusted at equivalent bacterial density, were plated on solid 7H11 medium containing various concentrations of isoniazid, ethambutol, or rifampicin. For each strain and each antibiotic, a minimal inhibitory concentration yielding a 90% (MIC_{90}) decrease in the number of colony-forming units was calculated (Table 3). No significant difference in the MIC_{90} was observed between the recombinant strains from each series for any of the antibiotic tested. Thus, susceptibility to the major anti-tuberculous drugs was not affected by the *Rv2952*^{G526A} mutation.

Given the major role played by DIM and PGL in mycobacterial virulence (13, 26, 30), we investigated whether the structural modifications observed in Beijing strains contributed to the virulence of these strains. For this purpose, BALB/c mice were intranasally co-infected with a mixture of strains HN878:pMV361Hy and HN878:p2952wt or a mixture of strains 94-1707:pMV361Hy and 94-1707:p2952wt. Bacterial load was evaluated in the lungs and spleen at various time points (Fig. 7). To quantify differences in growth between strains, a competition index was determined by calculating the ratio of mutant *versus* wild-type bacteria. The two recombinant HN878 strains grew equally well in the lungs and spleen of infected mice (Fig. 7*A*), and the ratio of HN878:p2952wt to HN878:pMV361Hy remained unchanged throughout the experiment in both these organs (data not shown). Similar results were obtained for the strains derived from 94-1707 (Fig. 7*B* and data not shown). These mixed-infection experiments suggested that the *Rv2952*^{G526A} mutation did not confer a growth advantage in the mouse model. We also compared the multiplication of H37Rv and the H37Rv Δ*Rv2952*::*res* mutant strain. Again, we observed the same multiplication in lungs and spleen for the two strains (data not shown). These results showed that the change in DIM and PGL profile associated with a decrease or loss of Rv2952 activity does not significantly affect the ability to *M. tuberculosis* strain to multiply and persist within lungs and spleen.

Another phenotype associated with some Beijing strains is the

TABLE 3
MIC_{90} of INH, EMB and Rif for recombinant strains derived from HN878 and 94–1707

M. tuberculosis strain	MIC_{90}[a]		
	Isoniazid	Ethambutol	Rifampicin
		$\mu g \cdot ml^{-1}$	
HN878:p2952wt	0.07 ± 0.01	0.62 ± 0.08	1.33
HN878:p2952mu	0.07 ± 0.01	0.51 ± 0.02	0.7 ± 0.03
HN878:pMV361	0.07 ± 0.01	0.68 ± 0.12	0.67
94–1707:p2952wt	0.08 ± 0.00	0.56 ± 0.10	1.36 ± 0.44
94–1707:p2952mu	0.05 ± 0.01	0.82 ± 0.25	1.36 ± 0.23
94–1707:pMV361	0.07 ± 0.01	0.57 ± 0.04	1.69 ± 0.1

[a] The MIC_{90} values are the means ± S.D. of three independent experiments, except for Rifampicin with strains HN878:p2952wt and HN878:pMV361, for which only one experiment was performed.

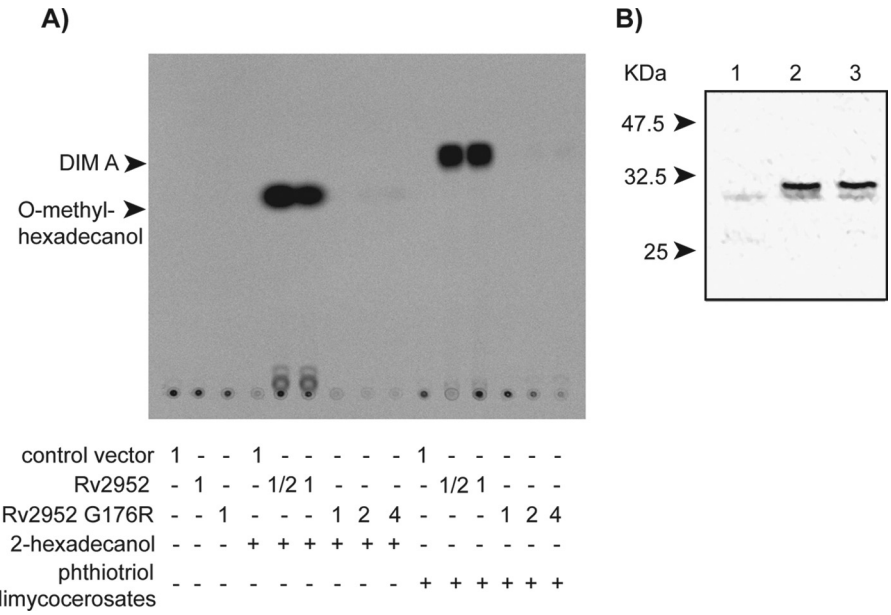

FIGURE 6. ***In vitro* enzymatic assay of Rv2952 and Rv2952 G176R proteins.** *A,* TLC analysis of the products formed after incubation of *E. coli* extracts containing either the empty vector or plasmid allowing expression of Rv2952 or Rv2952 G176R enzymes with the indicated substrates and *S*-[1-^{14}C]adenosylmethionine. *1* corresponded to 50 μl of *E. coli* extract (protein concentration: 5 mg·ml^{-1}); *½* corresponded to 25 μl of *E. coli* extract; *2* corresponded to 100 μl of *E. coli* extract; *4* corresponded to 200 μl of *E. coli* extract. The reaction products were separated by TLC and detected by autoradiography. *B,* Western blot analysis of protein extracts from *E. coli* expressing the *Rv2952* gene or the *Rv2952*^{G526A} allele. 12 μg of proteins from each strain were separated by SDS-PAGE (12% acrylamide/bisacrylamide 37.5:1) and transferred onto a nitrocellulose membrane. Wild-type or mutated Rv2952 proteins fused to His tag were revealed using anti-His antibody. *Lane 1,* extract from *E. coli* carrying the control vector; *lane 2*, extract from *E. coli* expressing the wild-type allele of *Rv2952*; *lane 3,* extract from *E. coli* expressing the *Rv2952*^{G526A} allele.

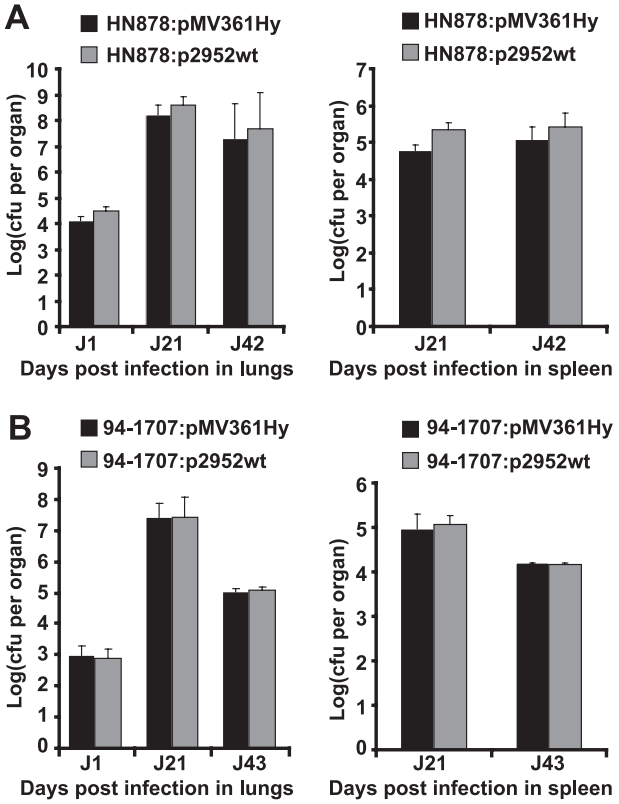

FIGURE 7. **Competition experiments in mice.** *A,* BALB/c mice were intranasally co-infected with HN878:pMV361Hy and HN878:p2952wt. *B,* BALB/c mice were intranasally co-infected with 94-1707:pMV361Hy and 94-1707:p2952wt. The number of cfu recovered at various time points from the lungs (*left panels*) and spleen (*right panels*) was evaluated by plating dilutions of homogenized tissues on 7H11 medium containing either Hyg (for cfu counts of the HN878:pMV361Hy and the 94-1707:pMV361Hy strains, *dark gray bars*) or Km (for cfu counts of the HN878:p2952wt and the 94-1707:p2952wt strains, *light gray bars*). The values shown are means ± S.D. (*error bars*) of cfu counts for three to five infected mice.

induction of a weaker inflammatory response upon the infection of mouse BMDM than induced by the laboratory strain H37Rv (13, 31). To test the possible relationship between this observation and the specific lipid profile of the Beijing strains, we compared the cytokine production by BMDM infected with wild-type or recombinant (HN878 and 94-1707) strains (Fig. 8). BMDM from B6D2 F1 mice were infected at multiplicity of infection of 5:1, and TNF-α, IL-12 p70, IL-10, and MCP1 were assayed from the supernatant 5 h after infection for TNF-α and 24 h after infection for the other cytokines. Too little IL-12p70 was produced for detection in these assays. As reported previously (13, 31), HN878 infection was associated with the release of smaller amounts of TNF-α and IL-10 than infection with H37Rv (Fig. 8*A*). In contrast, no significant difference in MCP-1 secretion following infection with H37Rv and HN878 was found in our assays (Fig. 8*A*). Comparisons of recombinant strains derived from HN878 showed no significant difference in TNF-α, IL-10, or MCP-1 production (Fig. 8*B*). In contrast to what was observed for HN878, infection with 94-1707 was not associated with lower levels of cytokine production than infection with H37Rv (Fig. 8*A*). Again, changes in the profile of DIM production did not influence TNF-α and MCP-1 production (Fig. 8*C*). However, infection with 94-1707:p2952wt was associated with a slightly higher level of IL-10 production than infection with 94-1707 or 94-1707:pMV361 (Fig. 8*C*). Altogether, these results indicate that the *Rv2952*^{G526A} mutation and the resulting changes in lipid profile were not associated with a drastic change in inflammatory cytokine production by infected cells. It remains, however, that the slightly different levels of IL-10 obtained with 94-1707:p2952wt compared with 94-1707 wild-type or 94-1707:pMV361 were reproducible and may thus suggest that the mutation might have slightly modified the cytokine response.

DISCUSSION

Here we show that Beijing strains of *M. tuberculosis* exhibit an unusual lipid profile, with the accumulation of structural variants of DIM and PGL not found in non-Beijing *M. tuberculosis* isolates. Our sequence analyses revealed that the single nucleotide change at position 526 of *Rv2952* was specific to the Beijing family. Indeed, the same mutation was identified in all 30 Beijing strains analyzed, which represent the various lineages of the Beijing family. In contrast, this mutation was not detected in other *M. tuberculosis* strains or in other *Mycobacterium* species producing DIM and PGL. These results strongly suggest that the nucleotide change at position 526 of *Rv2952* occurred in a common ancestor of the Beijing strains after the divergence of the *M. tuberculosis* species. The Gly to Arg mutation modifies a highly conserved residue and results in the replacement of a Gly residue by an Arg residue. Alignment of the Rv2952 sequence with other methyltransferases (data not shown) showed this mutation to affect the extremity of a conserved β-sheet involved in the canonical fold of *S*-adenosylmethionine-dependent methyltransferase (32). Although this mutation does not map close to the active site, it drastically impacts the *O*-methyltransferase activity of the Rv2952 protein *in vitro*. This finding and the gene complementation experiments unambiguously demonstrated that the G176R mutation was responsible for the unusual pattern of DIM and PGL production in Beijing strains.

The Rv2952 enzyme acts on phthiotriol and phenolphthiotriol chains, which are produced by the reduction of phthiodiolone and phenolphthiodiolone catalyzed by Rv2951c (Fig. 1*A*). Therefore, the accumulation of upstream biosynthetic intermediates as a consequence of alteration of Rv2952 function was expected (Fig. 1*A*). In contrast, the discovery of new accumulating compounds, acylated DIM and acylated PGL, in which the hydroxyl group of phthiotriol and phenolphthiotriol dimycocerosates is esterified with a palmitic acid, was more surprising. Acylated PGL was previously identified in our laboratory in a Δ*Rv2952* H37Rv mutant (27), but this compound and the acylated DIM have not previously been reported as natural products in field isolates of *M. tuberculosis*. The production of the triacylated compounds in a *null Rv2952* H37Rv mutant (27) showed that the acyltransferase activity is not due to a change in enzymatic function of Rv2952 induced by the G176R mutation. Another enzyme, which remains to be identified, must therefore be involved in the transfer of the third acyl residue onto the hydroxyl group.

The pattern of DIM production in Beijing strains is very different from that in other families of *M. tuberculosis*

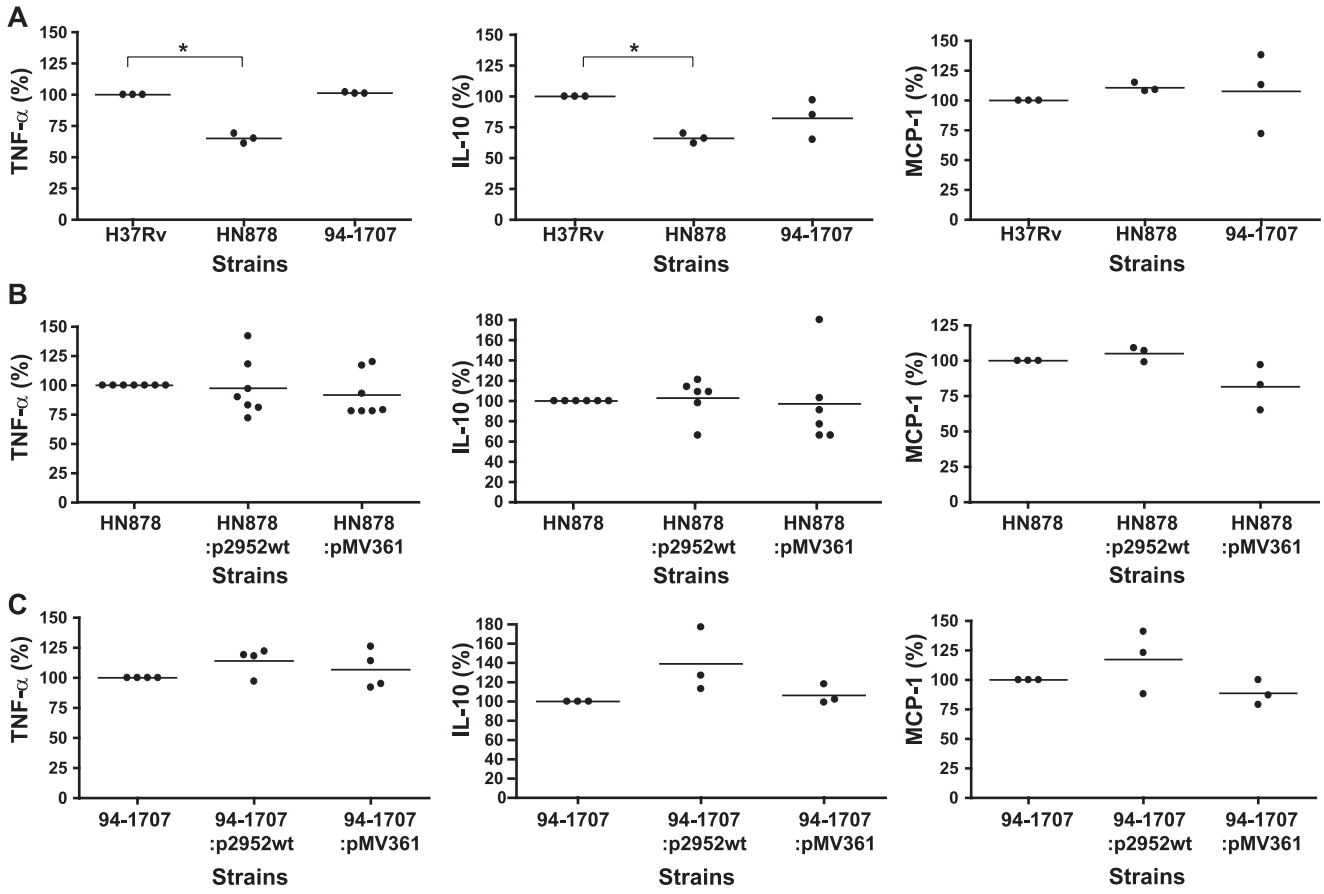

FIGURE 8. **Production of cytokines by BMDM infected with *M. tuberculosis* H37Rv and Beijing strains.** *A,* cytokine production after BMDM infection with H37Rv, HN878, or 94-1707 wild-type strains. *B,* cytokine production after BMDM infection with HN878 wild-type and derived strains. *C,* cytokine production after BMDM infection with 94-1707 wild-type and derived strains. Culture supernatants obtained 5 h after infection were analyzed by ELISA for the TNF-α secretion (*left panels*). Culture supernatants obtained 24 h after infection were analyzed by ELISA for the presence of the cytokines IL-10 and MCP-1 (*middle* and *right panels,* respectively). The values shown are the means of three to seven independent experiments performed in duplicate. *, $p < 0.05$.

strains, because of the *Rv2952*^{G526A} mutation. Indeed, DIM A are the major forms in non-Beijing isolates, whereas they are minor forms of DIM in 94-1707 and HN878. In contrast, DIM B and phthiotriol dimycocerosates are the predominant forms in Beijing strains. Similar observations may be made for PGL; PGL-tb is the major form, accounting for almost all the PGL synthesized in H37Rv:pPET1 and *M. canettii* (data not shown), whereas four forms of PGL are found in HN878. Given the known role of DIM in the permeability barrier formed by the cell envelope (29), we compared the resistance to the major anti-tuberculous drugs and to SDS of HN878 or 94-1707 strains expressing either the Beijing pattern of DIM and PGL or the H37Rv pattern. No significant difference was found between the strains within each series, suggesting that the various forms of DIM, and possibly PGL, fulfill similar roles as DIM A and PGL-tb in the cell envelope. These results are consistent with our recent finding that an H37Rv mutant deficient in DIM A synthesis but accumulating DIM B has no apparent defect in resistance to SDS (33). These results support the concept that there is some flexibility in the structure of DIM that does not prevent these molecules to achieve their structural function in the cell envelope. The most striking phenotypes associated with the Beijing strains include their greater capacity to multiply within mice (11, 34) and the weaker Th1-type immune response induced by these strains than by non-Beijing isolates (10, 31). We therefore evaluated the impact of the *Rv2952*^{G526A} mutation on these phenotypes. We first compared two series of recombinant strains derived from HN878 or 94-1707 and producing either the canonical patterns of DIM, possibly with PGL-tb, or the Beijing profile, in mixed-infection experiments. No significant difference was observed between the strains of each series, in terms of the capacity to multiply and to persist within the lungs of mice and to colonize the spleen. This lack of difference was reflected in the constant competitive index over the entire experiments. We then compared the amounts of TNF-α, IL10, and MCP1 cytokines produced by mouse BMDM infected with the HN878 or 94-1707 recombinant strains. Again no major difference was found between the recombinant strains within the same series. This was not because of a poor resolution of our assays because, as expected, the TNF-α response induced by H37Rv infection was clearly different from that induced by HN878, consistent with a previously described report (13). We therefore concluded that the *Rv2952*^{G526A} mutation and the resulting changes in DIM and PGL profiles had no major impact on the virulence of Beijing strains in the mouse model. As for the contribution of these lipids to cell envelope function, there seem to be some tolerance of structural flexibility

regarding the role of DIM and PGL in the interactions with the host.

Acknowledgments—We thank Dr. Clifton Barry III (Tuberculosis Research Section, National Institutes of Health) and Dr. Carlos Martin (Grupo de Genetica de Micobacterias, Universidad de Zaragoza, Spain) for providing us with strain HN878 and 1237, respectively. We are grateful several colleagues from the Institut de Pharmacologie et de Biologie Structurale (Toulouse, France) as follows: Dr. G. Tabouret for help with the mouse bone marrow-derived macrophages and helpful discussions; Drs. F. Laval and A. Lemassu for their technical assistance with mass spectrometry and NMR spectroscopy, respectively; Dr. V. Guillet for help with modeling of Rv2952 structure; and F. Viala for the contribution to figure preparation. Funding for the NMR spectrometers was obtained from the CNRS, the University Paul Sabatier, the Région Midi-Pyrénées, and the European Structural Funds.

REFERENCES

1. Caws, M., Thwaites, G., Dunstan, S., Hawn, T. R., Lan, N. T., Thuong N. T., Stepniewska, K., Huyen, M. N., Bang, N. D., Loc, T. H., Gagneux, S., van Soolingen, D., Kremer, K., van der Sande, M., Small, P., Anh, P. T., Chinh, N. T., Quy, H. T., Duyen, N. T., Tho, D. Q., Hieu, N. T., Torok, E., Hien, T. T., Dung, N. H., Nhu, N. T., Duy, P. M., van Vinh, Chau, N., and Farrar, J. (2008) *PloS Pathog.* **4,** e1000034
2. Malik, A. N., and Godfrey-Faussett, P. (2005) *Lancet Infect. Dis.* **5,** 174–183
3. Gagneux, S., and Small, P. M. (2007) *Lancet Infect. Dis.* **7,** 328–337
4. van Soolingen, D., Qian, L., de Haas, P. E., Douglas, J. T., Traore, H., Portaels, F., Qing, H. Z., Enkhsaikan, D., Nymadawa, P., and van Embden, J. D. (1995) *J. Clin. Microbiol.* **33,** 3234–3238
5. Kremer, K., Glynn, J. R., Lillebaek, T., Niemann, S., Kurepina, N. E., Kreiswirth, B. N., Bifani, P. J., and van Soolingen, D. (2004) *J. Clin. Microbiol.* **42,** 4040–4049
6. European Concerted Action on New Generation Genetic Markers and Techniques for the Epidemiology and Control of Tuberculosis (2006) *Emerg. Inf. Dis.* **12,** 736–743
7. Bifani, P. J., Plikaytis, B. B., Kapur, V., Stockbauer, K., Pan, X., Lutfey, M. L., Moghazeh, S. L., Eisner, W., Daniel, T. M., Kaplan, M. H., Crawford, J. T., Musser, J. M., and Kreiswirth, B. N. (1996) *JAMA* **275,** 452–457
8. Bifani, P. J., Mathema, B., Liu, Z., Moghazeh, S. L., Shopsin, B., Tempalski, B., Driscol, J., Frothingham, R., Musser, J. M., Alcabes, P., and Kreiswirth, B. N. (1999) *JAMA* **282,** 2321–2327
9. Caminero, J. A., Pena, M. J., Campos-Herrero, M. I., Rodríguez, J. C., García, I., Cabrera, P., Lafoz, C., Samper, S., Takiff, H., Afonso, O., Pavón, J. M., Torres, M. J., van Soolingen, D., Enarson, D. A., and Martin, C. (2001) *Am. J. Resp. Crit. Care Med.* **164,** 1165–1170
10. López, B., Aguilar, D., Orozco, H., Burger, M., Espitia, C., Ritacco, V., Barrera, L., Kremer, K., Hernandez-Pando, R., Huygen, K., and van Soolingen, D. (2003) *Clin. Exp. Immunol.* **133,** 30–37
11. Dormans, J., Burger, M., Aguilar, D., Hernandez-Pando, R., Kremer, K., Roholl, P., Arend, S. M., and van Soolingen, D. (2004) *Clin. Exp. Immunol.* **137,** 460–468
12. Manca, C., Tsenova, L., Bergtold, A., Freeman, S., Tovey, M., Musser, J. M., Barry, C. E., 3rd, Freedman, V. H., and Kaplan, G. (2001) *Proc. Natl. Acad. Sci. U.S.A.* **98,** 5752–5757
13. Reed, M. B., Domenech, P., Manca, C., Su, H., Barczak, A. K., Kreiswirth, B. N., Kaplan, G., and Barry, C. E., 3rd (2004) *Nature* **431,** 84–87
14. Kong, Y., Cave, M. D., Zhang, L., Foxman, B., Marrs, C. F., Bates, J. H., and Yang, Z. H. (2007) *J. Clin. Microbiol.* **45,** 409–414
15. Tsenova, L., Ellison, E., Harbacheuski, R., Moreira, A. L., Kurepina, N., Reed, M. B., Mathema, B., Barry, C. E., 3rd, and Kaplan, G. (2005) *J. Infect. Dis.* **192,** 98–106
16. Kremer, K., van der Werf, M. J., Au, B. K., Kam, K. M., van Doorn, H. R., Borgdroff, M. W., and van Soolingen, D. (2009) *Emerg. Inf. Dis.* **15,** 335–339
17. Constant, P., Perez, E., Malaga, W., Lanéelle, M. A., Saurel, O., Daffé, M., and Guilhot, C. (2002) *J. Biol. Chem.* **277,** 38148–38158
18. Daffé, M., and Laneelle, M. A. (1988) *J. Gen. Microbiol.* **134,** 2049–2055
19. Daffé, M., Lacave, C., Lanéelle, M. A., and Lanéelle, G. (1987) *Eur. J. Biochem.* **167,** 155–160
20. Malaga, W., Constant, P., Euphrasie, D., Cataldi, A., Daffé, M., Reyrat, J. M., and Guilhot, C. (2008) *J. Biol. Chem.* **283,** 15177–15184
21. Reed, M. B., Gagneux, S., Deriemer, K., Small, P. M., and Barry, C. E., 3rd (2007) *J. Bacteriol.* **189,** 2583–2589
22. Sinsimer, D., Huet, G., Manca, C., Tsenova, L., Koo, M. S., Kurepina, N., Kana, B., Mathema, B., Marras, S. A., Kreiswirth, B. N., Guilhot, C., and Kaplan, G. (2008) *Infect. Immun.* **76,** 3027–3036
23. Laval, F., Lanéelle, M. A., Déon, C., Monsarrat, B., and Daffé, M. (2001) *Anal. Chem.* **73,** 4537–4544
24. Daffé, M., and Draper, P. (1998) *Adv. Microb. Physiol.* **39,** 131–203
25. Guilhot, C., Chalut, C., and Daffé, M. (2008) in *The Mycobacterial Cell Envelope* (Daffé, M., and Reyrat, J. M., eds) pp. 273–289, American Society for Microbiology, Washington, D. C.
26. Camacho, L. R., Ensergueix, D., Perez, E., Gicquel, B., and Guilhot, C. (1999) *Mol. Microbiol.* **34,** 257–267
27. Pérez, E., Constant, P., Laval, F., Lemassu, A., Lanéelle, M. A., Daffé, M., and Guilhot, C. (2004) *J. Biol. Chem.* **279,** 42584–45592
28. Stover, C. K., de la Cruz, V. F., Fuerst, T. R., Burlein, J. E., Benson, L. A., Bennett, L. T., Bansal, G. P., Young, J. F., Lee, M. H., and Hatfull, G. F. (1991) *Nature* **351,** 456–460
29. Camacho, L. R., Constant, P., Raynaud, C., Laneelle, M. A., Triccas, J. A., Gicquel, B., Daffe, M., and Guilhot, C. (2001) *J. Biol. Chem.* **276,** 19845–19854
30. Cox, J. S., Chen, B., McNeil, M., and Jacobs, W. R., Jr. (1999) *Nature* **402,** 79–83
31. Manca, C., Reed, M. B., Freeman, S., Mathema, B., Kreiswirth, B., Barry, C. E., 3rd, and Kaplan, G. (2004) *Infect. Immun.* **72,** 5511–5514
32. Martin, J. L., and McMillan, F. M. (2002) *Curr. Opin. Struct. Biol.* **12,** 783–793
33. Siméone, R., Constant, P., Malaga, W., Guilhot, C., Daffé, M., and Chalut, C. (2007) *FEBS J.* **274,** 1957–1969
34. Barczak, A. K., Domenech, P., Boshoff, H. I., Reed, M. B., Manca, C., Kaplan, G., and Barry, C. E., 3rd (2005) *J. Infect. Dis.* **192,** 600–606